

Optogenetic activation of heterotrimeric G-proteins by LOV2GIVE, a rationally engineered modular protein

Mikel Garcia-Marcos*, Kshitij Parag-Sharma†, Arthur Marivin, Marcin Maziarz, Alex Luebbbers, Lien T Nguyen

Department of Biochemistry, Boston University School of Medicine, Boston, United States

Abstract Heterotrimeric G-proteins are signal transducers involved in mediating the action of many natural extracellular stimuli and many therapeutic agents. Non-invasive approaches to manipulate the activity of G-proteins with high precision are crucial to understand their regulation in space and time. Here, we developed LOV2GIVE, an engineered modular protein that allows the activation of heterotrimeric G-proteins with blue light. This optogenetic construct relies on a versatile design that differs from tools previously developed for similar purposes, that is metazoan opsins, which are light-activated G-protein-coupled receptors (GPCRs). Instead, LOV2GIVE consists of the fusion of a G-protein activating peptide derived from a non-GPCR regulator of G-proteins to a small plant protein domain, such that light uncages the G-protein activating module. Targeting LOV2GIVE to cell membranes allowed for light-dependent activation of Gi proteins in different experimental systems. In summary, LOV2GIVE expands the armamentarium and versatility of tools available to manipulate heterotrimeric G-protein activity.

*For correspondence: mgm1@bu.edu

Present address: †Graduate Curriculum in Cell Biology and Physiology, Biological and Biomedical Sciences Program, University of North Carolina, Chapel Hill, United States

Competing interests: The authors declare that no competing interests exist.

Funding: See page 13

Received: 18 June 2020

Accepted: 15 September 2020

Published: 16 September 2020

Reviewing editor: Volker Dötsch, Goethe University, Germany

© Copyright Garcia-Marcos et al. This article is distributed under the terms of the [Creative Commons Attribution License](https://creativecommons.org/licenses/by/4.0/), which permits unrestricted use and redistribution provided that the original author and source are credited.

Introduction

Heterotrimeric G-proteins are critical transducers of signaling triggered by a large family of G-protein-coupled receptors (GPCRs). GPCRs are Guanine nucleotide Exchange Factors (GEFs) that activate G-proteins by promoting the exchange of GDP for GTP on the G α -subunits (Gilman, 1987). This signaling axis regulates a myriad of (patho)physiological processes and also represents the target for >30% of drugs on the market (Sriram and Insel, 2018), which fuels the interest in developing tools to manipulate G-protein activity in cells with high precision.

Optogenetics, the use of genetically-encoded proteins to control biological processes with light (Warden et al., 2014), is well-suited for the non-invasive manipulation of signaling. Metazoan opsins are light-activated GPCRs that have been repurposed as optogenetic tools (Airan et al., 2009; Bailes et al., 2012; Karunathne et al., 2013; Oh et al., 2010; Siuda et al., 2015), albeit with limitations. For example, opsins tend to desensitize after activation due to receptor internalization and/or exhaustion of their chromophore, retinal (Airan et al., 2009; Bailes et al., 2012; Siuda et al., 2015). Exogenous supplementation of retinal, which is not always feasible, is required in many experimental settings because this chromophore is not readily synthesized by most mammalian cell types or by many organisms. Also, opsins are relatively large, post-translationally modified transmembrane proteins, which makes them inherently difficult to modify for optimization and/or customization for specific applications.

Here we leveraged the light-sensitive LOV2 domain of *Avena sativa* (Harper et al., 2003) to develop an optogenetic activator of heterotrimeric G-proteins not based on opsins. LOV2 uses ubiquitously abundant FMN as the chromophore and does not desensitize. It is small (~17 KDa) and expresses easily as a soluble globular protein in different systems (Lungu et al., 2012;

Strickland et al., 2012; Zayner et al., 2013), making it experimentally tractable, easily customizable, and widely applicable. Our results provide the proof-of-principle for a versatile optogenetic activator of heterotrimeric G-proteins that does not rely on GPCR-like proteins.

Results and discussion

Design and optimization of a photoswitchable G-protein activator

We envisioned the design of a genetically-encoded photoswitchable activator of heterotrimeric G-proteins by fusing a short sequence (~25 amino acids) from the protein GIV (a.k.a. Girdin) called the *G α -Binding-and-Activating* (GBA) motif to the C-terminus of LOV2 (**Figure 1A**, left). GBA motifs are evolutionarily conserved sequences found in various cytoplasmic, non-GPCR proteins that are sufficient to activate heterotrimeric G-protein signaling (*DiGiacomo et al., 2018*). We reasoned that the GBA motif would be 'uncaged' and bind G-proteins when the C-terminal $\text{J}\alpha$ -helix of LOV2 becomes disordered upon illumination (*Harper et al., 2003; Figure 1A*, right). We named this optogenetic construct LOV2GIV (pronounced 'love-to-give'). To facilitate the biochemical characterization of LOV2GIV, we initially used two well-validated mutants that mimic either the dark (D) or the lit (L) conformation of LOV2 (*Harper et al., 2004; Harper et al., 2003; Zimmerman et al., 2016; Figure 1A*, right), with the intent of subsequently validating the G-protein regulatory activity of LOV2GIVe in cells using light.

Our first LOV2GIV prototype had a suboptimal dynamic range, as it bound the G-protein $\text{G}\alpha\text{i}3$ in the lit conformation only ~3 times more than in the dark conformation (**Figure 1B**). Based on a structural homology model of LOV2GIV (**Figure 1C**), we reasoned that it could be due to the relatively high accessibility of $\text{G}\alpha\text{i}3$ -binding residues of the GIV GBA motif (L1682, F1685, L1686) within the dark conformation of LOV2GIV. In agreement with this idea, fusion of the GBA motif at positions of the $\text{J}\alpha$ helix more proximal to the core of the LOV2 domain tended to lower G-protein binding, including one variant ('e', henceforth referred to as LOV2GIVe) in which binding to the dark conformation was almost undetectable (**Figure 1D**). Consistent with this, a structure homology model of LOV2GIVe showed that amino acids required for G-protein binding are less accessible than in the LOV2GIV prototype (**Figure 1E**). In contrast, the lit conformation of LOV2GIVe displayed robust $\text{G}\alpha\text{i}3$ binding, thereby confirming an improved dynamic range compared to the LOV2GIV prototype (**Figure 1F**). Mutation of GIV's F1685 to alanine, a replacement known to preclude G-protein binding (*de Opakua et al., 2017; Garcia-Marcos et al., 2009*), resulted in greatly diminished binding of $\text{G}\alpha\text{i}3$ to the lit conformation of LOV2GIVe (**Figure 1—figure supplement 1**).

LOV2GIVe binds and activates G-proteins efficiently in vitro only in its lit conformation

Concentration-dependent binding curves revealed that the affinity of $\text{G}\alpha\text{i}3$ for the dark conformation of LOV2GIVe is orders of magnitude weaker than for the lit conformation (**Figure 2A**), which had an equilibrium dissociation constant (K_D) similar to that previously reported for the GIV- $\text{G}\alpha\text{i}3$ interaction (*DiGiacomo et al., 2017*). We also found that LOV2GIVe retains the same G-protein specificity as GIV. Much like GIV (*Garcia-Marcos et al., 2010; Marivin et al., 2020*), LOV2GIVe bound robustly only to members of the $\text{G}_{i/o}$ family among the four families of $\text{G}\alpha$ proteins ($\text{G}_{i/o}$, G_s , $\text{G}_{q/11}$, and $\text{G}_{12/13}$), and could discriminate within the $\text{G}_{i/o}$ family by binding to $\text{G}\alpha\text{i}1$, $\text{G}\alpha\text{i}2$ and $\text{G}\alpha\text{i}3$ but not to $\text{G}\alpha_o$ (**Figure 2B**). Next, we assessed if LOV2GIVe can activate G-proteins in vitro, that is whether it retains GIV's GEF activity. First, we measured $\text{G}\alpha\text{i}3$'s steady-state GTPase activity in the presence of LOV2GIVe to assess its GEF activity. Under steady-state conditions, nucleotide exchange is rate limiting because GTP hydrolysis occurs orders of magnitude faster than GTP loading for $\text{G}\alpha\text{i}$ proteins (*Mukhopadhyay and Ross, 2002*). Thus, steady-state GTP hydrolysis can report changes in the rate of nucleotide exchange on $\text{G}\alpha\text{i}$, which we have previously validated for GIV and other related non-receptor GEFs (*Aznar et al., 2015; Coleman et al., 2016; Garcia-Marcos et al., 2010; Garcia-Marcos et al., 2011*). We found that LOV2GIVe in the lit, but not the dark, conformation led to a dose-dependent increase of $\text{G}\alpha\text{i}3$ activity (**Figure 2C**), which was comparable to that previously shown for GIV (*Garcia-Marcos et al., 2009*). Using a GTP γ S binding assay that measures nucleotide exchange more directly, we also found that LOV2GIVe in the lit conformation promoted nucleotide exchange on $\text{G}\alpha\text{i}3$, an effect that was impaired upon introduction of the F1685A (FA) mutation that

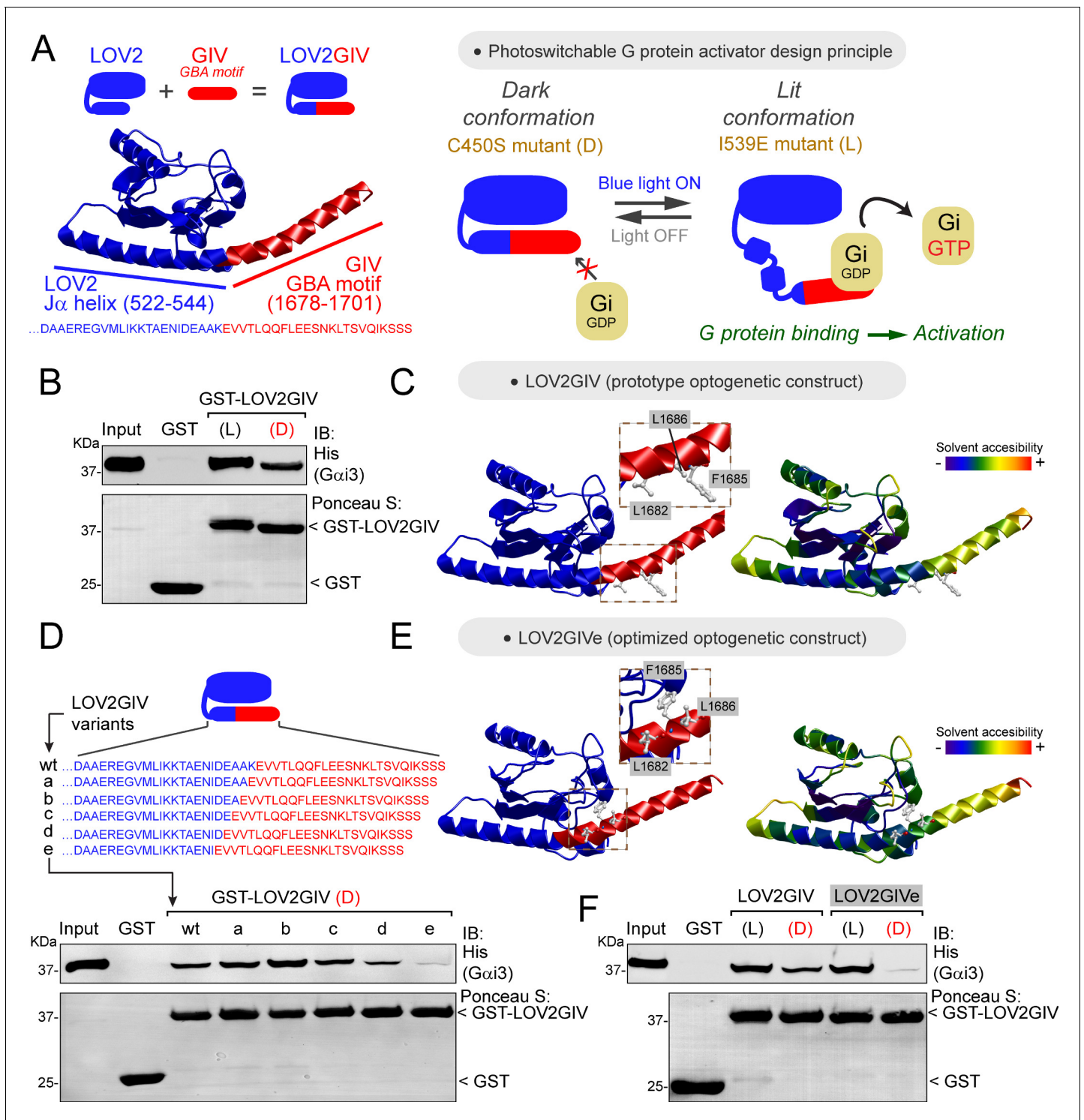


Figure 1. Design and optimization of LOV2GIV, an optogenetic activator of heterotrimeric G-proteins. (A) *Left*, diagram depicting the design of the LOV2GIV fusion protein. The GBA motif of GIV (red) is fused to the C-terminus of the LOV2 domain (blue). *Right*, diagram depicting the design principle of the photoswitchable G-protein activator LOV2GIV. In the dark conformation (D, which is mimicked by the LOV2 C450S mutant), the C-terminus of LOV2 forms an α -helix ($J\alpha$) and the GBA motif is not readily accessible for G-proteins. In the lit conformation (L, which is mimicked by the LOV2 mutant I539E), the C-terminus of LOV2 is more disordered and the GBA motif becomes accessible for G-proteins, which in turn are activated upon binding to the GBA motif. (B) LOV2GIV (L) binds G α i3 better than LOV2GIV (D). Approximately 20 μ g of the indicated purified GST-fused constructs were immobilized on glutathione-agarose beads and incubated with 3 μ g (~300 nM) of purified His-G α i3. Resin-bound proteins were eluted, separated by SDS-PAGE, and analyzed by Ponceau S-staining and immunoblotting (IB) with the indicated antibodies. Input = 10% of the total amount

Figure 1 continued on next page

Figure 1 continued

of His-G α i3 added in each binding reaction. (C) Ribbon representation of a LOV2GIV structure homology model generated using the I-TASSER server. On the left, the model is colored blue for LOV2 and red for GIV, whereas on the right it is colored according to solvent accessibility. Selected GIV residues known to be important for G-protein binding (L1682, F1685, L1686) (de Opakua et al., 2017; Kalogriopoulos et al., 2019) are displayed in stick representation and enlarged in the boxes. (D) LOV2GIV (D) variant 'e' displays greatly diminished G α i3 binding compared to LOV2GIV (D) wt. Protein binding experiments were carried out as described in panel B, except that the indicated LOV2GIV variants were used. (E) Ribbon representation of a structure homology model of the LOV2GIVe variant was generated and displayed as described for LOV2GIV in panel C. (F) The dynamic range of G α i3 binding to lit versus dark conformations is improved for LOV2GIVe compared to LOV2GIV. Protein binding experiments were carried out as described in panel B, except that the indicated LOV2GIV variants were used. For all protein binding experiments in this figure, one representative result of at least three independent experiments is shown.

The online version of this article includes the following figure supplement(s) for figure 1:

Figure supplement 1. FA mutation in LOV2GIVe (L) impairs G-protein binding.

reduces G-protein binding or when using the dark-mimicking mutant (D) of LOV2GIVe (Figure 2—figure supplement 1). These findings indicate that LOV2GIVe recapitulates the G-protein activating properties of GIV in vitro, and that these are effectively suppressed for the dark conformation.

LOV2GIVe activates G-protein signaling in cells in its lit conformation

To investigate LOV2GIVe-dependent G-protein activation in cells, we initially used a humanized yeast-based system (Cismowski et al., 1999; DiGiacomo et al., 2020) in which the mating pheromone response pathway has been co-opted to measure activation of human G α i3 using a gene reporter (LacZ, β -galactosidase activity) (Figure 3A, left). When we expressed LOV2GIVe dark (D), lit (L) or wt in this strain, only very weak levels of β -galactosidase activity were detected (Figure 3A, right). We reasoned that this could be due to the subcellular localization of the construct, presumed to be cytosolic in the absence of any targeting sequence, because we have previously shown that GIV requires membrane localization to efficiently activate G-proteins (Parag-Sharma et al., 2016). Expressing LOV2GIVe (L) fused to a membrane-targeting sequence (mLOV2GIVe) led to a very strong induction of β -galactosidase activity, which was not recapitulated by expression of mLOV2GIVe (D) or wt (Figure 3A, right). LOV2GIVe-mediated activation levels (several hundred-fold over basal) are comparable to those previously reported for the endogenous pathway in response to GPCR activation by mating pheromone (Hoffman et al., 2002; Lambert et al., 2010). Next, we tested mLOV2GIVe in mammalian cells. Instead of using a downstream signaling readout as we did in yeast, we used a Bioluminescence Resonance Energy Transfer (BRET) biosensor that measures G-protein activity directly (Figure 3B, left). Expression of mLOV2GIVe (L), but not (D), led to an increase of BRET proportional to the amount of plasmid transfected (Figure 3B, right). At the highest amount tested, mLOV2GIVe (L) caused a BRET increase comparable to that observed upon maximal stimulation of the M4 muscarinic receptor, a Gi-activating GPCR (Figure 3B, right, Figure 3—figure supplement 1). Introducing a mutation that precludes G-protein activation by GIV's GBA motif (F1685A (FA), [Garcia-Marcos et al., 2009]), in mLOV2GIVe (L) also abolished its ability to induce a BRET increase (Figure 3—figure supplement 2). As an alternative readout of G-protein regulation by LOV2GIVe, we measured cAMP levels in cells because the enzymes that produce this second messenger, adenylyl cyclases, are classical effectors of GTP-bound G α i subunits. Acute activation of Gi proteins leads to inhibition of adenylyl cyclase activity, but prolonged Gi activation leads to the opposite effect— it sensitizes adenylyl cyclases to subsequent activating inputs, such as the stimulation of a Gs-linked GPCR, leading to the potentiation of cAMP production (Brust et al., 2015; Watts and Neve, 2005). We found that expression of LOV2GIVe (L) leads to a potentiation of the cAMP response induced by the β -adrenergic agonist isoproterenol, suggesting prolonged activation of Gi proteins in cells (Figure 3—figure supplement 3). The magnitude of the potentiation (~2 fold) is comparable to that reported for many Gi-activating GPCRs (Watts and Neve, 2005). In contrast, expression of similar amounts of LOV2GIVe (L) bearing the F1685A (FA) mutation or of LOV2GIVe (D), which do not bind or activate G α i, failed to recapitulate the potentiation of the cAMP response elicited by LOV2GIV (L) (Figure 3—figure supplement 3), further supporting the involvement of G α i activation. Taken together, our results indicate that the lit conformation of LOV2GIVe activates G-protein signaling in different cell types.

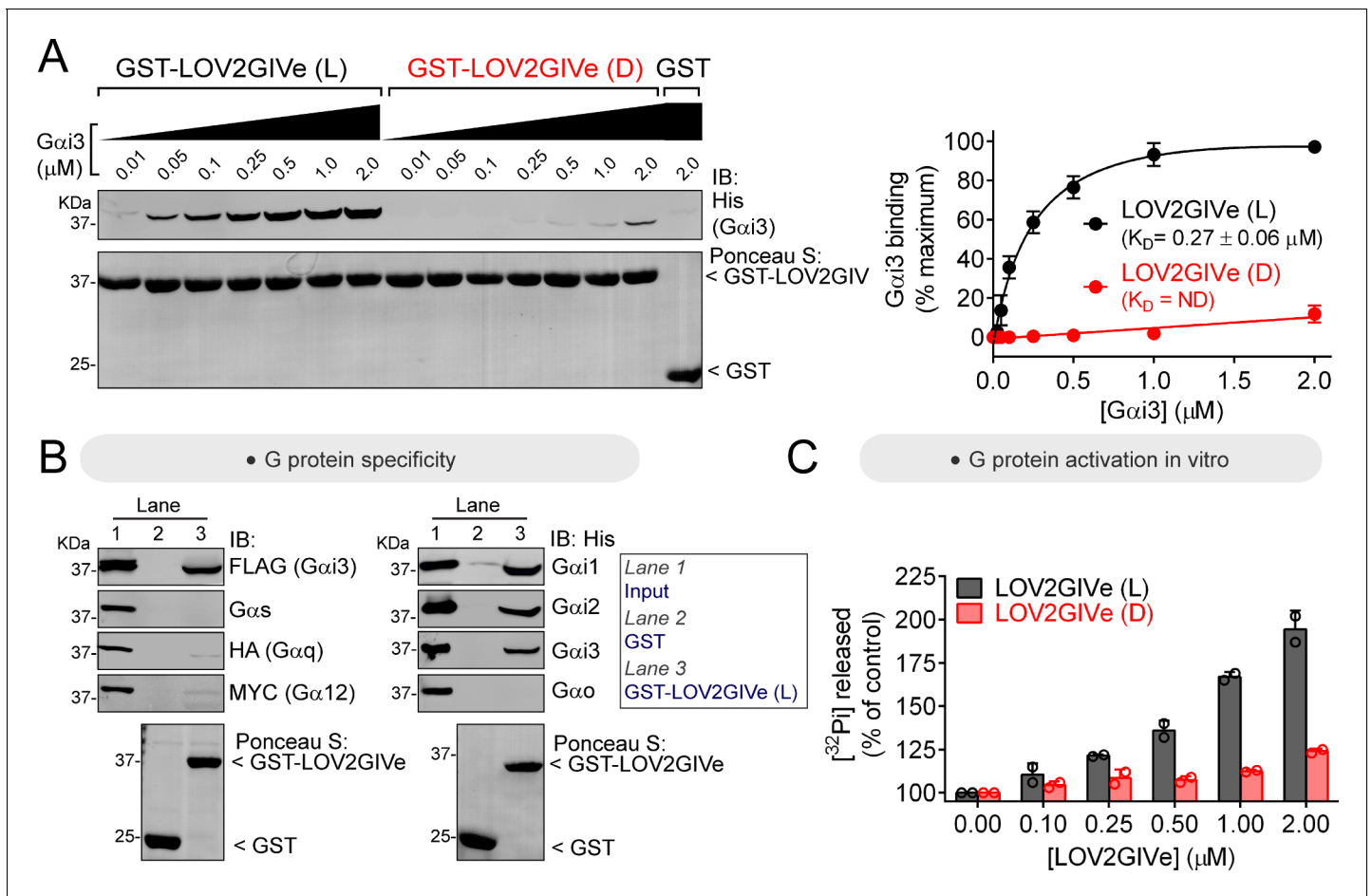


Figure 2. LOV2GIVe binds and activates Gαi3 in vitro in its lit conformation. (A) LOV2GIVe binds with high affinity to Gαi3. Approximately 10 μg of the indicated purified GST-fused constructs were immobilized on glutathione-agarose beads and incubated with the indicated concentrations of purified His-Gαi3. Resin-bound proteins were eluted, separated by SDS-PAGE, and analyzed by Ponceau S-staining and immunoblotting (IB) with the indicated antibodies. One representative result is shown on the left, and the graph on the right corresponds to the quantification of three independent experiments presented as mean ± S.E.M. for each data point and a solid line for the fit to a single site binding curve used to determine the K_D values. (B) LOV2GIVe binds specifically to Gαi compared to other Gα subunits. Approximately 20 μg of the indicated purified GST-fused constructs were immobilized on glutathione-agarose beads and incubated with the lysates of HEK293T cells expressing the indicated G-proteins (FLAG-Gαi3, Gαs, Gαq-HA and Gα12-MYC on the left panels) or purified His-tagged proteins (3 μg, ~300 nM of His-Gαi1, His-Gαi2, His-Gαi3 and His-Gαo on the right panels). One representative experiment of at least three is shown. (C) LOV2GIVe (L), but not LOV2GIVe (D), increases Gαi3 activity in vitro. Steady-state GTPase activity of purified His-Gαi3 was determined in the presence of increasing amounts (0–2 μM) of purified GST-LOV2GIVe (L) (black) or GST-LOV2GIVe (D) (red) by measuring the production of [³²P]Pi at 15 min. Results are the mean ± S.D. of n = 2. The online version of this article includes the following source data and figure supplement(s) for figure 2:

Source data 1. Numerical data used for panel A.

Source data 2. Numerical data used for panel C.

Figure supplement 1. LOV2GIVe (L) promotes GTP binding to Gαi3 in vitro.

Figure supplement 1—source data 1. Numerical data used to generate the graph.

LOV2GIVe activates G-protein signaling in cells upon illumination

Next, we tested whether LOV2GIVe can trigger G-protein activation in cells in response to light. For this, we used two complementary experimental systems. The first one consisted of measuring G-protein activity directly with the mammalian cell BRET biosensor described above upon illumination with a pulse of blue light. We found that, in HEK293T cells expressing mLOV2GIVe wt, a single short light pulse resulted in a spike of G-protein activation that decayed at a rate similar to that reported for the transition from lit to dark conformation of LOV2 ($T_{1/2} \sim 1$ min) (Figure 4A). This response was not recapitulated by a mLOV2GIVe construct bearing the GEF-deficient FA mutation (Figure 4A). For

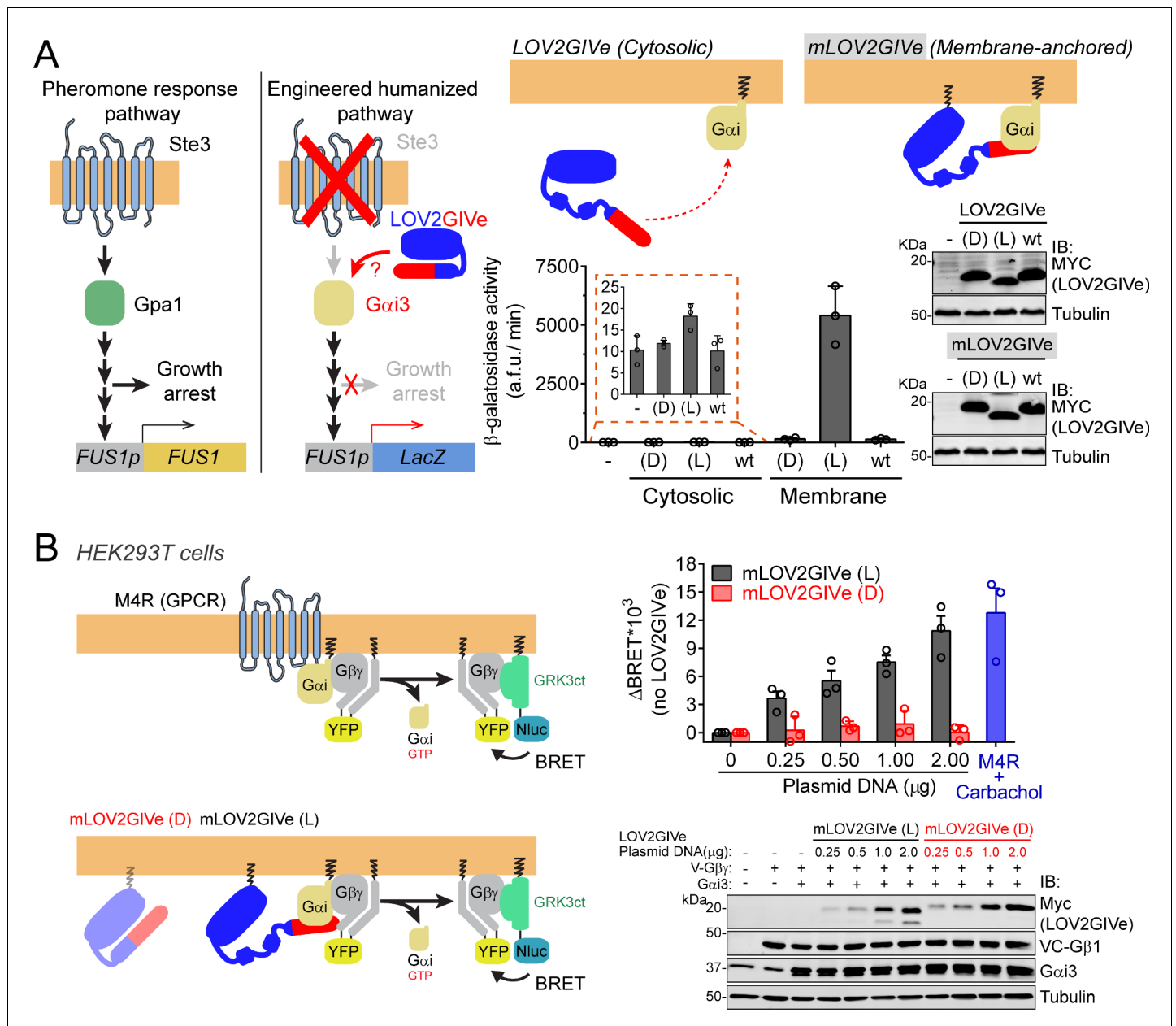


Figure 3. LOV2GIVe activates G-protein signaling in cells in its lit conformation. (A) *Left*, diagram comparing key steps and components of the mating pheromone response pathway of *Saccharomyces cerevisiae* to those of an engineered, humanized strain used in the experiments shown in this figure. In the engineered strain, no pheromone responsive GPCR (Ste3) is expressed, the yeast G-protein Gpa1 is replaced by human Gai3, and downstream signaling does not lead to growth arrest but promotes the activation of a reporter gene (*LacZ*) under the control of the pheromone-sensitive, G-protein-dependent promoter of *FUS1* (*FUS1p*). *Right*, membrane-anchored LOV2GIVe (mLOV2GIVe), but not its untargeted parental version, leads to strong G-protein activation only in the lit conformation. Yeast strains expressing the indicated LOV2GIVe constructs ((D), (L) or wt) or an empty vector (-) were lysed to determine β -galactosidase activity using a fluorogenic substrate (mean \pm S.E.M., $n = 3$) and to prepare samples for immunoblotting (IB) (one experiment representative of 3 is shown). (B) *Left*, diagrams showing the principle for the G-protein activity biosensor used in this panel. Upon action of a GPCR (top) or mLOV2GIVe (bottom), G-protein activation leads to the release of YFP-tagged G $\beta\gamma$ from Gai, which then can associate with Nluc-tagged GRK3ct and results in the subsequent increase in BRET. *Right*, mLOV2GIVe (L) but not mLOV2GIVe (D), leads to increased G-protein activation similar to a GPCR as determined by BRET. BRET was measured in HEK293T cells transfected with the indicated amounts of mLOV2GIVe plasmid constructs along with the components of the BRET biosensor and the GPCR M4R. M4R was stimulated with 100 μ M carbachol. Results in the graph on the top are expressed as difference in BRET (Δ BRET) relative to unstimulated cells not expressing mLOV2GIVe (mean \pm S.E.M., $n = 3$). One representative immunoblot from cell lysates made after the BRET measurements is shown on the bottom. The online version of this article includes the following source data and figure supplement(s) for figure 3:

Source data 1. Numerical data used for panel A.

Figure 3 continued on next page

Figure 3 continued

Source data 2. Numerical data used for panel B.

Figure supplement 1. Carbachol dose-dependent G-protein activation and its blockade by atropine.

Figure supplement 1—source data 1. Numerical data used to generate the graph.

Figure supplement 2. FA mutation abolishes G-protein activation by mLOV2GIVE (L) in cells.

Figure supplement 2—source data 1. Numerical data used to generate the graph.

Figure supplement 3. LOV2GIVE (L) expression enhances isoproterenol-induced cAMP levels in cells via Gi regulation.

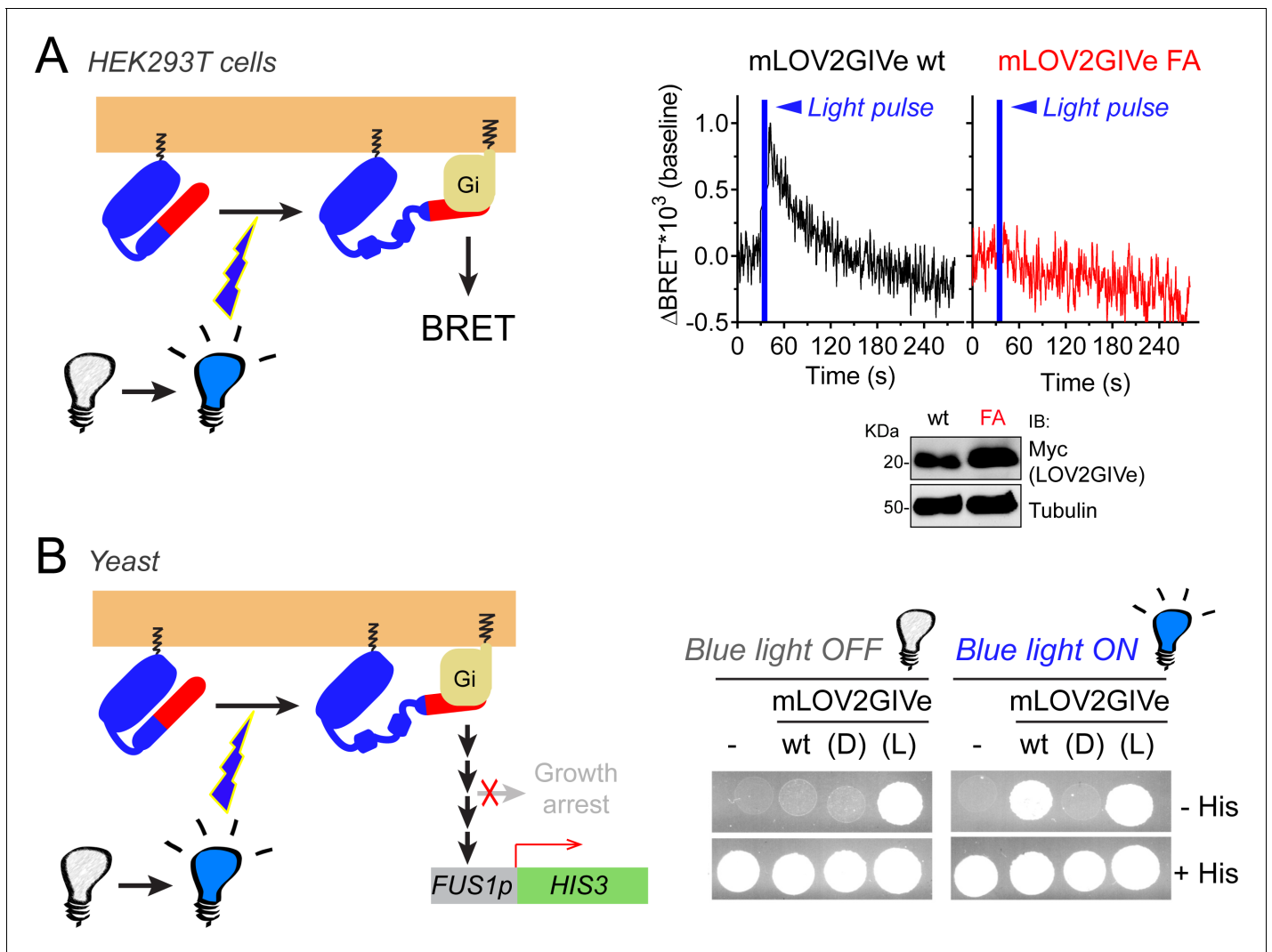
Figure supplement 3—source data 1. Numerical data used for panel A.

Figure supplement 3—source data 2. Numerical data used for panel B.

the second system, we turned to the humanized yeast strain described above. Instead of using β -galactosidase assays to report G-protein dependent activation of the *FUS1* promoter by light, we assayed conditional histidine prototrophy controlled by the *FUS1* promoter using spot growth assays because they are better suited to allow homogenous and continued illumination than the cell suspension conditions used of the β -galactosidase assay (**Figure 4B**, left). Yeast cells expressing mLOV2GIVE wt grew in the absence of histidine only when exposed to blue light (**Figure 4B**, right). This effect was specifically caused by light-dependent activation of mLOV2GIVE wt because cells expressing the light-insensitive mLOV2GIVE (D) construct failed to grow under the same illumination conditions, whereas mLOV2GIVE (L) grew the same regardless of illumination conditions (**Figure 4B**, right). Taken together, these results show that mLOV2GIVE activates G-protein signaling in cells upon blue light illumination.

Conclusions and future perspectives

Here, we have presented proof-of-principle evidence for a photoswitchable G-protein activator that does not rely on opsins, that is light-activated GPCRs. This tool is based on a modular design that combines the properties of the light-sensitive LOV2 domain with a motif present in a non-GPCR activator of G-proteins of the Gi family. We propose that the versatility of the LOV2GIVE design could help overcome some limitations of currently available optogenetic tools that are based on GPCR-like proteins. For example, recent evidence suggests that opioid receptors can activate Gi proteins in different subcellular compartments (**Stoeber et al., 2018**), but it has not been possible to control GPCR activation in specific subcellular compartments to address the consequences of spatially encoded signals. Given that our results indicate that LOV2GIVE requires targeting to membranes where the substrate G-protein localizes (**Figure 3A**), it would be possible in the future to target it to different membranous organelles to trigger Gi activation in specific subcellular compartments. LOV2GIVE could also be useful for neurobiological applications because Gi proteins are critical mediator of inhibitory neuromodulation. Combined with the potential for subcellular compartmentalization, LOV2GIVE could be leveraged to assess the different impact of inhibitory modulation at pre- or post-synaptic sites. Our results also support that LOV2GIVE can activate G-protein signaling even in cellular systems where there is not sufficient synthesis of retinal to support opsin-based activation, like in the yeast *S. cerevisiae* (**Scott et al., 2019**). This could open the application of optogenetic Gi activation to organisms or experimental settings in which the lack of external supplementation of retinal is detrimental, such those required prolonged and/or repeated stimulation. A general advantage of optogenetic approaches over other synthetic biology approaches to activate G-proteins like chemogenetics with Designer Receptors Exclusively Activated by Designer Drugs (DREADDs) (**Urban and Roth, 2015**) is that they allow for the rapid and accurate temporal control of both activation and deactivation. Thus, LOV2GIVE could be used to investigate Gi signaling processes over a broad temporal scale, also including intermittent or pulsatile activation. A limitation of LOV2GIVE is that it only acts on one subset of heterotrimeric G-proteins, those containing G α i subunits. Nevertheless, potential applications are still broad, as Gi proteins control processes as diverse as inhibitory neuromodulation, opioid action, or heart rate, among many others.



Materials and methods

Reagents and antibodies

Unless otherwise indicated, all chemical reagents were obtained from Sigma or Fisher Scientific. Fluorescein di- β -D-galactopyranoside (FDG) was from Marker Gene Technologies, and the protein inhibitor mixture was from Sigma (catalog no. S8830). Leupeptin, pepstatin, and aprotinin were from Gold Biotechnology. All restriction endonucleases and *E. coli* strain BL21(DE3) were from Thermo Scientific. *E. coli* strain DH5 α was purchased from New England Biolabs. *Pfu* ultra DNA polymerase used for site-directed mutagenesis was purchased from Agilent. [γ - 32 P]GTP was from Perkin Elmer. Mouse monoclonal antibodies raised against α -tubulin (T6074), FLAG tag (F1804) or His-tag (H1029) were from Sigma. Mouse monoclonal antibody raised against hemagglutinin (HA) tag (clone 12CA5, #11583816001) was obtained from Roche. Mouse monoclonal antibody raised against MYC-tag

(9B11, #2276) was from Cell Signaling. Rabbit polyclonal antibody raised against G α s (C-18, sc-383) was purchased from Santa Cruz Biotechnology. Goat anti-rabbit Alexa Fluor 680 (A21077) and goat anti-mouse IRDye 800 (#926–32210) secondary antibodies were from Life technologies and LiCor, respectively.

Plasmid constructs

The parental LOV2GIV sequence was obtained as a synthetic gene fragment from GenScript and subsequently amplified by PCR with extensions at the 5' and 3' ends that made it compatible with a ligation-independent cloning (LIC) system (Stols *et al.*, 2002). For the bacterial expression of GST-LOV2GIV constructs, we inserted the LOV2GIV sequence into the pLIC-GST plasmid kindly provided by J. Sondek (UNC-Chapel Hill) (Cabrita *et al.*, 2006) to generate the plasmid pLIC-GST-LOV2GIV. Two previously described LOV2 mutations (L514K and L531E) that reduce the spurious unwinding of the J α helix in the dark conformation (Lungu *et al.*, 2012; Zimmerman *et al.*, 2016) were introduced in this construct. These and other mutations to generate the dark (D, C450S) and lit (L, I539E) conformations, the a, b, c, d, and e variants described on Figure 1D, and the GEF-deficient FA mutant were made using the QuikChange II Mutagenesis Kit from Agilent. Full sequences of the parental LOV2GIV and LOV2GIVe variant are provided in Supplementary Information. For the yeast expression of LOV2GIVe constructs, we inserted the LOV2GIVe sequence into two different versions of a previously described pYES2 derived plasmid (Coleman *et al.*, 2016): pLIC-YES2 and pLIC-YES2-N9Gpa1. Both versions contain a MYC-tag sequence cloned upstream of the LIC cassette between the HindIII and KpnI sites, but in one of the two plasmids it was preceded by a sequence encoding the first nine amino acids of *S. cerevisiae* Gpa1, a previously validated membrane-targeting sequence (Parag-Sharma *et al.*, 2016; Song *et al.*, 1996). For the mammalian expression of LOV2GIVe constructs, we inserted the LOV2GIVe sequence into a modified pLIC-myc plasmid (Cabrita *et al.*, 2006, kindly provided by J. Sondek (UNC-Chapel Hill, NC)), in which a sequence encoding the first 11 amino acids of Lyn, a previously validated membrane-targeting sequence (Inoue *et al.*, 2005; Parag-Sharma *et al.*, 2016), was inserted in the AflIII/KpnI sites upstream of the MYC-tag (pLIC-lyn11-myc). The resulting sequence preceding the first amino acid of LOV2GIVe is **MGCIKSKGKDSGTELGSMEQKLISEEDLGILYFOSNA** (bold = Lyn11, underline = MYC-tag). Cloning of the pET28b-G α i3 and pET28b-G α o plasmids for the bacterial expression of rat His-G α i3 or rat His-G α o (isoform A), respectively, have been described previously (Garcia-Marcos *et al.*, 2010; Garcia-Marcos *et al.*, 2009). Plasmid pLIC-G α i1(int.6xHis) for the bacterial expression of rat G α i1 with an internal hexahistidine tag at position 120 was generated by PCR amplification from pQE6-G α i1(int.6xHis) (Dessauer *et al.*, 1998, kindly provided by Carmen Dessauer, University of Texas, Houston) and insertion at NdeI/BglII sites of the pLIC-His plasmid (Stols *et al.*, 2002). The plasmid for the bacterial expression of rat His-G α i2 (pET28b-G α i2) was generated by inserting the G α i2 sequence into the NdeI/EcoRI of pET28b. Plasmids for expression of FLAG-G α i3 (rat, p3XFLAG-CMV10-G α i3, N-terminal 3XFLAG tag) or G α s (human, pcDNA3.1(+)-G α s) in mammalian cells were described previously (Beas *et al.*, 2012; Garcia-Marcos *et al.*, 2009). Plasmids for the expression of G α q-HA (mouse, pcDNA3-G α q-HA, internally tagged) or G α 12-MYC (mouse, pcDNA3.1-G α 12-MYC, internally tagged) in mammalian cells were kindly provided by P. Wedegaertner (Thomas Jefferson University) (Wedegaertner *et al.*, 1993) and T. Meigs (University of North Carolina, Asheville) (Ritchie *et al.*, 2013), respectively. Plasmid for the expression of G β 1 and G γ 2 fused to a split Venus (pcDNA3.1-Venus(1-155)-G γ 2 (VN-G γ 2) and pcDNA3.1-Venus(155-239)-G β 1 (VC-G β 1)) or for untagged G β 1 (pcDNA3.1-G β 1) and G γ 2 (pcDNA3.1-G γ 2) were kindly provided by N. Lambert (Augusta University, GA) (Hollins *et al.*, 2009). pcDNA3.1-masGRK3ct-Nluc and pcDNA3.1-Nluc-EPAC-VV (Masuho *et al.*, 2015) were a gift from K. Martemyanov (Scripps Research Institute, FL). The pcDNA3-G α i3 plasmid for the expression of rat G α i3 in mammalian cells has been described previously (Garcia-Marcos *et al.*, 2010; Garcia-Marcos *et al.*, 2009). The plasmid for the expression of M4R was obtained from the cDNA Resource Center at Bloomsburg University (pcDNA3.1-3xHA-M4R, cat# MAR040TN00).

Protein expression and purification

All His-tagged and GST-tagged proteins were expressed in BL21(DE3) *E. coli* transformed with the corresponding plasmids by overnight induction at 23°C with 1 mM isopropyl- β -D-1-thio-

galactopyranoside (IPTG). Protein purification was carried out following previously described protocols (*Garcia-Marcos et al., 2010; Garcia-Marcos et al., 2009*). Briefly, bacteria pelleted from 1 L of culture were resuspended in 25 mL of buffer [50 mM NaH₂PO₄, pH 7.4, 300 mM NaCl, 10 mM imidazole, 1% (v:v) Triton X-100 supplemented with protease inhibitor cocktail (Leupeptin 1 μM, Pepstatin 2.5 μM, Aprotinin 0.2 μM, PMSF 1 mM)]. For His-Gαi3 and His-Gαo, this buffer was supplemented with 25 μM GDP and 5 mM MgCl₂. After sonication (four cycles, with pulses lasting 20 s/cycle, and with 1 min interval between cycles to prevent heating), lysates were centrifuged at 12,000 g for 20 min at 4°C. The soluble fraction (supernatant) of the lysate was used for affinity purification on HisPur cobalt or glutathione- agarose resins (Pierce) and eluted with lysis buffer supplemented with 250 mM imidazole or with 50 mM Tris-HCl, pH 8, 100 mM NaCl, 30 mM reduced glutathione, respectively. GST-tagged proteins were dialyzed overnight at 4°C against PBS. For His-Gαi1, His-Gαi2, His-Gαi3 and His-Gαo, the buffer was exchanged for 20 mM Tris-HCl, pH 7.4, 20 mM NaCl, 1 mM MgCl₂, 1 mM DTT, 10 μM GDP, 5% (v/v) glycerol using a HiTrap Desalting column (GE Healthcare). All protein samples were aliquoted and stored at –80°C.

Protein–protein binding assays

GST pulldown assays were carried out as described previously (*Garcia-Marcos et al., 2010; Garcia-Marcos et al., 2011*) with minor modifications. GST or GST-fused LOV2GIV constructs (described in 'Plasmid Constructs') were immobilized on glutathione-agarose beads for 90 min at room temperature in PBS. Beads were washed twice with PBS, resuspended in 250–400 μL of binding buffer (50 mM Tris-HCl, pH 7.4, 100 mM NaCl, 0.4% (v:v) NP-40, 10 mM MgCl₂, 5 mM EDTA, 1 mM DTT, 30 μM GDP) and incubated 4 hr at 4°C with constant tumbling in the presence of His-tagged G-proteins purified as described in 'Protein Expression and Purification' or lysates of HEK293T cells expressing different G-proteins. For the latter, HEK293T cells (ATCC CRL3216) were grown at 37°C, 5%CO₂ in high-glucose Dulbecco's Modified Eagle Medium (DMEM) supplemented with 10% FBS, 100 U/mL penicillin, 100 μg/mL streptomycin and 1% L-glutamine. HEK293T cells were not authenticated by STR profiling or tested for mycoplasma contamination. Approximately two million HEK293T cells were seeded on 10 cm dishes and transfected the day after using the calcium phosphate method with plasmids encoding the following constructs (DNA amounts in parenthesis): FLAG-Gαi3 (3 μg), Gαs (3 μg), Gαq-HA (6 μg) or Gα12-MYC (3 μg). Cell medium was changed 6 hr after transfection. Thirty two hours after transfection, cells were harvested by scraping in PBS and centrifugation before resuspension in 500 μL of ice-cold lysis buffer (20 mM HEPES, pH 7.2, 125 mM K(CH₃COO), 0.4% (vol:vol) Triton X-100, 1 mM DTT, 10 mM β-glycerophosphate and 0.5 mM Na₃VO₄ supplemented with a protease inhibitor cocktail [SigmaFAST, #S8830]). Cell lysates were cleared by centrifugation at 14,000 g for 10 min at 4°C. Approximately, 20–25% of the lysate from a 10 cm dish was used for each binding reaction. After incubation with purified proteins or cell lysates, beads were washed four times with 1 mL of wash buffer (4.3 mM Na₂HPO₄, 1.4 mM KH₂PO₄, pH 7.4, 137 mM NaCl, 2.7 mM KCl, 0.1% (v/v) Tween-20, 10 mM MgCl₂, 5 mM EDTA, 1 mM DTT, and 30 μM GDP) and resin-bound proteins eluted by boiling for 5 min in Laemmli sample buffer before processing for IB (see below 'Immunoblotting').

Protein structure modeling and visualization

Models of LOV2GIV and LOV2GIVe were generated using the server I-TASSER (<https://zhanglab.ccmb.med.umich.edu/I-TASSER/>, [Yang et al., 2015]). Best scoring models were chosen for further analysis (LOV2GIV C-score = –0.64, LOV2GIVe C-score = –0.33). Protein structures were visualized and displayed using ICM version 3.8–3 (Molsoft LLC., San Diego, CA).

Steady-state GTPase assay

This assay was performed as described previously (*Garcia-Marcos et al., 2010; Garcia-Marcos et al., 2009; Garcia-Marcos et al., 2011*). Briefly, His-Gαi3 (400 nM) was pre-incubated with different concentrations of GST-LOV2GIVe constructs for 15 min at 30°C in assay buffer [20 mM Na-HEPES, pH 8, 100 mM NaCl, 1 mM EDTA, 25 mM MgCl₂, 1 mM DTT, 0.05% (w:v) C₁₂E₁₀]. GTPase reactions were initiated at 30°C by adding an equal volume of assay buffer containing 1 μM [γ-³²P] GTP (~50 c.p.m/ fmol). Duplicate aliquots (25 μL) were removed at 15 min and reactions stopped with 975 μL of ice-cold 5% (w/v) activated charcoal in 20 mM H₃PO₄, pH 3. Samples were then

centrifuged for 10 min at 10,000 g, and 500 μ L of the resultant supernatant were scintillation counted to quantify [32 P]Pi released. Background [32 P]Pi detected at 15 min in the absence of G-protein was subtracted from each reaction and data expressed as percentage of the Pi produced by His-G α i3 in the absence of GST-LOV2GIVe. Background counts were <5% of the counts detected in the presence of G-proteins.

GTP γ S binding assay

GTP γ S binding to purified His-G α i3 was determined as described previously (*Garcia-Marcos et al., 2010; Leyme et al., 2014*). Purified His-G α i3 (100 nM) was diluted in assay buffer (20 mM Na-HEPES, pH 8, 100 mM NaCl, 1 mM EDTA, 25 mM MgCl₂, 1 mM DTT, 0.05% (wt:vol) C₁₂E₁₀) and pre-incubated with purified GST-LOV2GIVe proteins (2 μ M final) for 15 min at 30°C. Reactions were initiated, by adding an equal volume of assay buffer containing 1 μ M [35 S]GTP γ S (~50 c.p.m./ fmol) at 30°C. Duplicate aliquots (25 μ L) were removed 15 min after the reaction start, and binding of radioactive nucleotide was stopped by addition of 2 mL of ice-cold wash buffer (20 mM Tris-HCl, pH 8.0, 100 mM NaCl, 25 mM MgCl₂). The quenched reactions were rapidly passed through BA-85 nitrocellulose filters (GE Healthcare) and washed with 2 mL cold wash buffer. Filters were dried and subjected to liquid scintillation counting. Background [35 S]GTP γ S detected in the absence of G-protein was subtracted from each reaction and data expressed as percentage of the [35 S]GTP γ S bound to His-G α i3 in the absence of GST-LOV2GIVe.

Yeast strains and manipulations

The previously described (*Cismowski et al., 1999*) *S. cerevisiae* strain CY7967 [*MAT α GPA1(1–41)-Gai3 far1 Δ fus1p-HIS3 can1 ste14:trp1:LYS2 ste3 Δ lys2 ura3 leu2 trp1 his3*] (kindly provided by James Broach, Penn State University) was used for all yeast experiments. The main features of this strain are that the gene encoding only pheromone responsive GPCR (*STE3*) is deleted, the endogenous G α -subunit Gpa1 is replaced by a chimeric Gpa1(1-41)-human G α i3 (36-354) and the gene encoding the cell cycle arrest-inducing protein Far1 is deleted. In this strain, the pheromone response pathway can be upregulated by the ectopic expression of activators of human G α i3 and does not result in the cell cycle arrest that occurs in the native pheromone response (*Cismowski et al., 2002; Cismowski et al., 1999; Maziarz et al., 2018*). Plasmid transformations were carried out using the lithium acetate method. CY7967 was first transformed with a centromeric plasmid (CEN TRP) encoding the *LacZ* gene under the control of the *FUS1* promoter (*FUS1p*), which is activated by the pheromone response pathway. The *FUS1p::LacZ*-expressing strain was transformed with pLIC-YES2 plasmids (2 μ m, URA) encoding each of the LOV2GIV constructs described in 'Plasmid Constructs'. Double transformants were selected in synthetic defined (SD)-TRP-URA media. Individual colonies were inoculated into 3 mL of SDGalactose-TRP-URA and incubated overnight at 30°C to induce the expression of the proteins of interest under the control of the galactose-inducible promoter of pLIC-YES2. This starting culture was used to inoculate 20 mL of SDGalactose-TRP-URA at 0.3 OD₆₀₀. Exponentially growing cells (~0.7–0.8 OD₆₀₀, 4–5 hr) were pelleted to prepare samples for ' β -galactosidase Activity Assay' and 'Yeast Spot Growth Assay' described below and for preparing samples for immunoblotting as previously described (*de Opakua et al., 2017; Maziarz et al., 2018*). Briefly, pellets corresponding to 5 OD₆₀₀ were washed once with PBS + 0.1% BSA and resuspended in 150 μ L of lysis buffer (10 mM Tris-HCl, pH 8.0, 10% (w:v) trichloroacetic acid (TCA), 25 mM NH₄OAc, 1 mM EDTA). 100 μ L of glass beads were added to each tube and vortexed at 4°C for 5 min. Lysates were separated from glass beads by poking a hole in the bottom of the tubes followed by centrifugation onto a new set of tubes. The process was repeated after the addition of 50 μ L of lysis buffer to wash the glass beads. Proteins were precipitated by centrifugation (10 min, 20,000 g) and resuspended in 60 μ L of solubilization buffer (0.1 M Tris-HCl, pH 11.0, 3% SDS). Samples were boiled for 5 min, centrifuged (1 min, 20,000 g), and 50 μ L of the supernatant transferred to new tubes containing 12.5 μ L of Laemmli sample buffer and boiled for 5 min.

β -galactosidase activity assay

This assay was performed as described previously (*Hoffman et al., 2002; Maziarz et al., 2018*) with minor modifications. Pellets corresponding to 0.5 OD₆₀₀ (in duplicates) were washed once with PBS + 0.1% (w:v) BSA and resuspended in 200 μ L assay buffer (60 mM Na₂PO₄, 40 mM NaH₂PO₄, 10

mM KCl, 1 mM MgCl₂, 0.25% (v:v) β-mercaptoethanol, 0.01% (w:v) SDS, 10% (v:v) chloroform) and vortexed. 100 μL were transferred to 96-well plates and reactions started by the addition of 50 μL of the fluorogenic β-galactosidase substrate fluorescein di-β-D-galactopyranoside (FDG, 100 μM final). Fluorescence (Ex. 485 ± 10 nm/ Em. 528 ± 10 nm) was measured every 2 min for 90 min at 30°C in a Biotek H1 synergy plate reader. Enzymatic activity was calculated as arbitrary fluorescent units (a.f. u.) per minute (min).

BRET-based G-protein activation assay

BRET experiments were conducted as described previously (Maziarz et al., 2018). HEK293T cells (ATCC, CRL-3216) were seeded on 6-well plates (~400,000 cells/well) coated with gelatin and after one day transfected using the calcium phosphate method with plasmids encoding for the following constructs (DNA amounts in parenthesis): Venus(155-239)-Gβ₁ (VC-Gβ₁) (0.2 μg), Venus(1-155)-Gγ₂ (VN-Gγ₂) (0.2 μg) and Gαi3 (1 μg) mas-GRK3ct-Nluc (0.2 μg) along with mLOV2GIVE constructs in the amounts indicated in the corresponding figure legends. Approximately 16–24 hr after transfection, cells were washed and gently scraped in room temperature PBS, centrifuged (5 min at 550 g) and resuspended in assay buffer (140 mM NaCl, 5 mM KCl, 1 mM MgCl₂, 1 mM CaCl₂, 0.37 mM NaH₂PO₄, 20 mM HEPES pH 7.4, 0.1% glucose) at a concentration of 1 million cells/mL. 25,000–50,000 cells were added to a white opaque 96-well plate (Opti-Plate, Perkin Elmer) and mixed with the nanoluciferase substrate Nano-Glo (Promega cat# N1120, final dilution 1:200) for 2 min before measuring luminescence signals in a POLARstar OMEGA plate reader (BMG Labtech) at 28°C. Luminescence was measured at 460 ± 40 nm and 535 ± 10 nm, and BRET was calculated as the ratio between the emission intensity at 535 ± 10 nm divided by the emission intensity at 460 ± 40 nm. For the activation of M4R in Figure 3B, cells were exposed to 100 μM carbachol for 4 min prior to measuring BRET. For measurements shown in Figure 3B and Figure 4B, BRET data are presented as the difference from cells not expressing LOV2GIVE constructs. For kinetic BRET measurements shown in Figure 4A, luminescence signals were measured every 0.24 s for the duration of the experiment. The illumination pulse was achieved by switching from the luminescence read mode to the fluorescence read mode of the plate reader, with the following settings: 485 ± 6 nm filter, 200 flashes (~1.5 s). After the pulse of illumination, measurements were returned to luminescence mode with the same settings as prior to illumination. BRET data were corrected by subtracting the BRET signal baseline (average of 30 s pre-light pulse) and then subjected to a smoothing function (second order, four neighbors) in GraphPad for presentation. At the end of some BRET experiments, a separate aliquot of the same pool of cells used for the luminescence measurements was centrifuged for 1 min at 14,000 g and pellets stored at –20°C. To prepare lysates for IB, pellets were resuspended in lysis buffer (20 mM HEPES, pH 7.2, 5 mM Mg(CH₃COO)₂, 125 mM K(CH₃COO), 0.4% Triton X-100, 1 mM DTT, and protease inhibitor mixture). After clearing by centrifugation at 14,000 g at 4°C for 10 min, protein concentration was determined by Bradford and samples boiled in Laemmli sample buffer for 5 min before following the procedures described in 'Immunoblotting'.

Intracellular cAMP measurements

This assay was performed using the previously described BRET-based biosensor NLuc-EPAC-VV (Leyme et al., 2017; Masuho et al., 2015). HEK293T cells were seeded, transfected, and harvested as described above ('BRET-based G-protein activation assay') except that the plasmids used were (quantities in parenthesis): NLuc-EPAC-VV (0.05 μg), Gαi3 (1 μg) Gβ1 (0.5 μg), Gγ2 (0.5 μg) and the mLOV2GIVE constructs indicated in the figures (2 μg). A POLARstar OMEGA plate reader (BMG Labtech) was used to measure luminescence signals at 460 ± 20 nm and 528 ± 10 nm at 28°C every 5 s and BRET calculated as the ratio between the emission intensity at 528 ± 10 nm divided by the emission intensity at 460 ± 20 nm. Results were normalized to the basal BRET ratio before the addition of isoproterenol and presented as the inverse of this normalized BRET ratio. Isoproterenol (0.1 μM) was added at 60 s. Preparation of protein samples for IB was performed as described in 'BRET-based G-Protein Activation Assay'.

Yeast spot growth assay

Cells bearing LOV2GIVE constructs growing exponentially in SDGalactose media were pelleted as described above ('Yeast Strains and Manipulations'), and resuspended at equal densities. Equal

volumes of each strain were spotted on agar plates in four identical sets. Two of the sets were seeded on SDGalactose-TRP-URA plates with histidine and the other two sets were seeded on SDGalactose-TRP-URA-HIS (supplemented with 5 mM 3-amino-1,2,4-triazole). From each one of the two pairs of sets, one of the plates was exposed to a homemade array of blue LED strips positioned approximately 12 cm above the plates (~2,000 Lux as determined by a Trendbox Digital Light Meter HS1010A) whereas the other one was incubated side by side under the same light but tightly wrapped in aluminum foil. Plates were incubated simultaneously under these conditions for 4 days at 30°C and then imaged using an Epson flatbed scanner.

Immunoblotting

Proteins were separated by SDS-PAGE and transferred to PVDF membranes, which were blocked with 5% (w:vol) non-fat dry milk and sequentially incubated with primary and secondary antibodies. For protein-protein binding experiments with GST-fused proteins, PVDF membranes were stained with Ponceau S and scanned before blocking. The primary antibodies used were the following: MYC (1:1,000), His (1:2,500), FLAG (1:2,000), α -tubulin (1:2,500), HA (1:1,000) and Gas (1:500). The secondary antibodies were goat anti-rabbit Alexa Fluor 680 (1:10,000) and goat anti-mouse IRDye 800 (1:10,000). Infrared imaging of immunoblots was performed using an Odyssey Infrared Imaging System (Li-Cor Biosciences). Images were processed using the ImageJ software (NIH) and assembled for presentation using Photoshop and Illustrator softwares (Adobe).

Acknowledgements

This work was supported by NIH grant R01GM136132 (to MG-M). MM was supported by an American Cancer Society - Funding Hope Postdoctoral Fellowship, PF-19-084-01-CDD. We thank N Lambert (Augusta University), K Martemyanov (The Scripps Research Institute, Florida), C Dessauer (University of Texas, Houston), J Sondek (University of North Carolina-Chapel Hill), P Wedegaertner (Thomas Jefferson University), and T Meigs (University of North Carolina-Asheville) for providing the plasmids.

Additional information

Funding

Funder	Grant reference number	Author
National Institute of General Medical Sciences	R01GM136132	Mikel Garcia-Marcos
American Cancer Society	PF-19-084-01-CDD	Marcin Maziarz

The funders had no role in study design, data collection and interpretation, or the decision to submit the work for publication.

Author contributions

Mikel Garcia-Marcos, Conceptualization, Formal analysis, Supervision, Funding acquisition, Investigation, Visualization, Methodology, Writing - original draft, Project administration, Writing - review and editing; Kshitij Parag-Sharma, Arthur Marivin, Marcin Maziarz, Formal analysis, Investigation, Writing - review and editing; Alex Luebbbers, Formal analysis, Investigation; Lien T Nguyen, Investigation

Author ORCIDs

Mikel Garcia-Marcos  <https://orcid.org/0000-0001-9513-4826>

Kshitij Parag-Sharma  <https://orcid.org/0000-0003-3638-0941>

Alex Luebbbers  <http://orcid.org/0000-0001-7733-4250>

Decision letter and Author response

Decision letter <https://doi.org/10.7554/eLife.60155.sa1>

Author response <https://doi.org/10.7554/eLife.60155.sa2>

Additional files

Supplementary files

- Supplementary file 1. Sequences of LOV2GIV constructs.
- Transparent reporting form

Data availability

All data generated or analysed during this study are included in the manuscript and supporting files. Source data files have been provided for Figures 2, 3 and 4 (and their corresponding supplements).

References

- Airan RD, Thompson KR, Fenno LE, Bernstein H, Deisseroth K. 2009. Temporally precise in vivo control of intracellular signalling. *Nature* **458**:1025–1029. DOI: <https://doi.org/10.1038/nature07926>, PMID: 19295515
- Aznar N, Midde KK, Dunkel Y, Lopez-Sanchez I, Pavlova Y, Marivin A, Barbazán J, Murray F, Nitsche U, Janssen KP, Willert K, Goel A, Abal M, Garcia-Marcos M, Ghosh P. 2015. Daple is a novel non-receptor GEF required for trimeric G protein activation in wnt signaling. *eLife* **4**:e07091. DOI: <https://doi.org/10.7554/eLife.07091>, PMID: 26126266
- Bailes HJ, Zhuang LY, Lucas RJ. 2012. Reproducible and sustained regulation of galphas signalling using a metazoan opsin as an optogenetic tool. *PLOS ONE* **7**:e30774. DOI: <https://doi.org/10.1371/journal.pone.0030774>, PMID: 22292038
- Beas AO, Taupin V, Teodorof C, Nguyen LT, Garcia-Marcos M, Farquhar MG. 2012. Galphas promotes EEA1 endosome maturation and shuts down proliferative signaling through interaction with GIV (Girdin). *Molecular Biology of the Cell* **23**:4623–4634. DOI: <https://doi.org/10.1091/mbc.E12-02-0133>, PMID: 23051738
- Brust TF, Conley JM, Watts VJ. 2015. Gαi/o-coupled receptor-mediated sensitization of adenylyl cyclase: 40 years later. *European Journal of Pharmacology* **763**:223–232. DOI: <https://doi.org/10.1016/j.ejphar.2015.05.014>
- Cabrita LD, Dai W, Bottomley SP. 2006. A family of *E. coli* expression vectors for laboratory scale and high throughput soluble protein production. *BMC Biotechnology* **6**:12. DOI: <https://doi.org/10.1186/1472-6750-6-12>, PMID: 16509985
- Cismowski MJ, Takesono A, Ma C, Lizano JS, Xie X, Fuernkranz H, Lanier SM, Duzic E. 1999. Genetic screens in yeast to identify mammalian nonreceptor modulators of G-protein signaling. *Nature Biotechnology* **17**:878–883. DOI: <https://doi.org/10.1038/12867>
- Cismowski MJ, Takesono A, Ma C, Lanier SM, Duzic E. 2002. Identification of modulators of mammalian G-protein signaling by functional screens in the yeast *Saccharomyces cerevisiae*. *Methods in Enzymology* **344**:153–168. DOI: [https://doi.org/10.1016/s0076-6879\(02\)44712-x](https://doi.org/10.1016/s0076-6879(02)44712-x), PMID: 11771380
- Coleman BD, Marivin A, Parag-Sharma K, DiGiacomo V, Kim S, Pepper JS, Casler J, Nguyen LT, Koelle MR, Garcia-Marcos M. 2016. Evolutionary conservation of a GPCR-Independent mechanism of trimeric G protein activation. *Molecular Biology and Evolution* **33**:820–837. DOI: <https://doi.org/10.1093/molbev/msv336>, PMID: 26659249
- de Opakua AI, Parag-Sharma K, DiGiacomo V, Merino N, Leyme A, Marivin A, Villate M, Nguyen LT, de la Cruz-Morcillo MA, Blanco-Canosa JB, Ramachandran S, Baillie GS, Cerione RA, Blanco FJ, Garcia-Marcos M. 2017. Molecular mechanism of galphai activation by non-GPCR proteins with a Galpha-Binding and activating motif. *Nature Communications* **8**:15163. DOI: <https://doi.org/10.1038/ncomms15163>, PMID: 28516903
- Dessauer CW, Tesmer JJ, Sprang SR, Gilman AG. 1998. Identification of a galpha binding site on type V adenylyl cyclase. *The Journal of Biological Chemistry* **273**:25831–25839. DOI: <https://doi.org/10.1074/jbc.273.40.25831>, PMID: 9748257
- DiGiacomo V, de Opakua AI, Papakonstantinou MP, Nguyen LT, Merino N, Blanco-Canosa JB, Blanco FJ, Garcia-Marcos M. 2017. The Galphai-GIV binding interface is a druggable protein-protein interaction. *Scientific Reports* **7**:8575. DOI: <https://doi.org/10.1038/s41598-017-08829-7>, PMID: 28819150
- DiGiacomo V, Marivin A, Garcia-Marcos M. 2018. When heterotrimeric G proteins are not activated by G Protein-Coupled receptors: structural insights and evolutionary conservation. *Biochemistry* **57**:255–257. DOI: <https://doi.org/10.1021/acs.biochem.7b00845>, PMID: 29035513
- DiGiacomo V, Maziarz M, Luebbbers A, Norris JM, Laksono P, Garcia-Marcos M. 2020. Probing the mutational landscape of regulators of G protein signaling proteins in Cancer. *Science Signaling* **13**:eaax8620. DOI: <https://doi.org/10.1126/scisignal.aax8620>, PMID: 32019900
- Garcia-Marcos M, Ghosh P, Farquhar MG. 2009. GIV is a nonreceptor GEF for G alpha i with a unique motif that regulates akt signaling. *PNAS* **106**:3178–3183. DOI: <https://doi.org/10.1073/pnas.0900294106>, PMID: 19211784
- Garcia-Marcos M, Ghosh P, Ear J, Farquhar MG. 2010. A structural determinant that renders G alpha(i) sensitive to activation by GIV/girdin is required to promote cell migration. *The Journal of Biological Chemistry* **285**:12765–12777. DOI: <https://doi.org/10.1074/jbc.M109.045161>, PMID: 20157114

- Garcia-Marcos M**, Kietsunthorn PS, Wang H, Ghosh P, Farquhar MG. 2011. G protein binding sites on calnuc (nucleobindin 1) and NUCB2 (nucleobindin 2) define a new class of G(alpha)-regulatory motifs. *The Journal of Biological Chemistry* **286**:28138–28149. DOI: <https://doi.org/10.1074/jbc.M110.204099>, PMID: 21653697
- Gilman AG**. 1987. G proteins: transducers of receptor-generated signals. *Annual Review of Biochemistry* **56**:615–649. DOI: <https://doi.org/10.1146/annurev.bi.56.070187.003151>, PMID: 3113327
- Harper SM**, Neil LC, Gardner KH. 2003. Structural basis of a phototropin light switch. *Science* **301**:1541–1544. DOI: <https://doi.org/10.1126/science.1086810>, PMID: 12970567
- Harper SM**, Christie JM, Gardner KH. 2004. Disruption of the LOV-Jalpha Helix interaction activates phototropin kinase activity. *Biochemistry* **43**:16184–16192. DOI: <https://doi.org/10.1021/bi048092i>, PMID: 15610012
- Hoffman GA**, Garrison TR, Dohlman HG. 2002. Analysis of RGS proteins in *Saccharomyces cerevisiae*. *Methods in Enzymology* **344**:617–631. DOI: [https://doi.org/10.1016/s0076-6879\(02\)44744-1](https://doi.org/10.1016/s0076-6879(02)44744-1), PMID: 11771415
- Hollins B**, Kuravi S, Digby GJ, Lambert NA. 2009. The c-terminus of GRK3 indicates rapid dissociation of G protein heterotrimers. *Cellular Signalling* **21**:1015–1021. DOI: <https://doi.org/10.1016/j.cellsig.2009.02.017>, PMID: 19258039
- Inoue T**, Heo WD, Grimley JS, Wandless TJ, Meyer T. 2005. An inducible translocation strategy to rapidly activate and inhibit small GTPase signaling pathways. *Nature Methods* **2**:415–418. DOI: <https://doi.org/10.1038/nmeth763>, PMID: 15908919
- Kalogriopoulos NA**, Rees SD, Ngo T, Kopcho NJ, Ilatovskiy AV, Sun N, Komives EA, Chang G, Ghosh P, Kufareva I. 2019. Structural basis for GPCR-independent activation of heterotrimeric gi proteins. *PNAS* **116**:16394–16403. DOI: <https://doi.org/10.1073/pnas.1906658116>, PMID: 31363053
- Karunaratne WK**, Giri L, Kalyanaraman V, Gautam N. 2013. Optically triggering spatiotemporally confined GPCR activity in a cell and programming neurite initiation and extension. *PNAS* **110**:E1565–E1574. DOI: <https://doi.org/10.1073/pnas.1220697110>, PMID: 23479634
- Lambert NA**, Johnston CA, Cappell SD, Kuravi S, Kimple AJ, Willard FS, Siderovski DP. 2010. Regulators of G-protein signaling accelerate GPCR signaling kinetics and govern sensitivity solely by accelerating GTPase activity. *PNAS* **107**:7066–7071. DOI: <https://doi.org/10.1073/pnas.0912934107>, PMID: 20351284
- Leyme A**, Marivin A, Casler J, Nguyen LT, Garcia-Marcos M. 2014. Different biochemical properties explain why two equivalent Gα subunit mutants cause unrelated diseases. *Journal of Biological Chemistry* **289**:21818–21827. DOI: <https://doi.org/10.1074/jbc.M114.549790>, PMID: 24982418
- Leyme A**, Marivin A, Maziarz M, DiGiacomo V, Papakonstantinou MP, Patel PP, Blanco-Canosa JB, Walawalkar IA, Rodriguez-Davila G, Dominguez I, Garcia-Marcos M. 2017. Specific inhibition of GPCR-independent G protein signaling by a rationally engineered protein. *PNAS* **114**:E10319–E10328. DOI: <https://doi.org/10.1073/pnas.1707992114>, PMID: 29133411
- Lungu OI**, Hallett RA, Choi EJ, Aiken MJ, Hahn KM, Kuhlman B. 2012. Designing photoswitchable peptides using the AsLOV2 domain. *Chemistry & Biology* **19**:507–517. DOI: <https://doi.org/10.1016/j.chembiol.2012.02.006>, PMID: 22520757
- Marivin A**, Maziarz M, Zhao J, DiGiacomo V, Calvo O, Mann EA, Ear J, Blanco-Canosa JB, Ross EM, Ghosh P. 2020. DAPLE protein inhibits nucleotide exchange on galphas and galphaq via the same motif that activates galphai. *The Journal of Biological Chemistry* **295**:2270–2284. DOI: <https://doi.org/10.1074/jbc.RA119.011648>
- Masuhō I**, Ostrovskaya O, Kramer GM, Jones CD, Xie K, Martemyanov KA. 2015. Distinct profiles of functional discrimination among G proteins determine the actions of G protein-coupled receptors. *Science Signaling* **8**:ra123. DOI: <https://doi.org/10.1126/scisignal.aab4068>, PMID: 26628681
- Maziarz M**, Broselid S, DiGiacomo V, Park JC, Luebbbers A, Garcia-Navarrete L, Blanco-Canosa JB, Baillie GS, Garcia-Marcos M. 2018. A biochemical and genetic discovery pipeline identifies PLCdelta4b as a nonreceptor activator of heterotrimeric G-proteins. *The Journal of Biological Chemistry* **293**:16964–16983. DOI: <https://doi.org/10.1074/jbc.RA118.003580>, PMID: 30194280
- Mukhopadhyay S**, Ross EM. 2002. Quench-flow kinetic measurement of individual reactions of G-protein-catalyzed GTPase cycle. *Methods in Enzymology* **344**:350–369. DOI: [https://doi.org/10.1016/s0076-6879\(02\)44727-1](https://doi.org/10.1016/s0076-6879(02)44727-1), PMID: 11771396
- Oh E**, Maejima T, Liu C, Deneris E, Herlitz S. 2010. Substitution of 5-HT1A receptor signaling by a light-activated G protein-coupled receptor. *The Journal of Biological Chemistry* **285**:30825–30836. DOI: <https://doi.org/10.1074/jbc.M110.147298>, PMID: 20643652
- Parag-Sharma K**, Leyme A, DiGiacomo V, Marivin A, Broselid S, Garcia-Marcos M. 2016. Membrane recruitment of the Non-receptor protein GIV/Girdin (Gα-interacting, Vesicle-associated protein/Girdin) Is sufficient for activating heterotrimeric G protein signaling. *Journal of Biological Chemistry* **291**:27098–27111. DOI: <https://doi.org/10.1074/jbc.M116.764431>
- Ritchie BJ**, Smolski WC, Montgomery ER, Fisher ES, Choi TY, Olson CM, Foster LA, Meigs TE. 2013. Determinants at the N- and C-termini of Gα₁₂ required for activation of Rho-mediated signaling. *Journal of Molecular Signaling* **8**:3. DOI: <https://doi.org/10.1186/1750-2187-8-3>
- Scott BM**, Chen SK, Bhattacharyya N, Moalim AY, Plotnikov SV, Heon E, Peisajovich SG, Chang BSW. 2019. Coupling of human rhodopsin to a yeast signaling pathway enables characterization of mutations associated with retinal disease. *Genetics* **211**:597–615. DOI: <https://doi.org/10.1534/genetics.118.301733>, PMID: 30514708
- Siuda ER**, McCall JG, Al-Hasani R, Shin G, Il Park S, Schmidt MJ, Anderson SL, Planer WJ, Rogers JA, Bruchas MR. 2015. Optodynamic simulation of β-adrenergic receptor signalling. *Nature Communications* **6**:8480. DOI: <https://doi.org/10.1038/ncomms9480>, PMID: 26412387

- Song J**, Hirschman J, Gunn K, Dohlman HG. 1996. Regulation of membrane and subunit interactions by N-myristoylation of a G protein alpha subunit in yeast. *The Journal of Biological Chemistry* **271**:20273–20283. DOI: <https://doi.org/10.1074/jbc.271.34.20273>, PMID: 8702760
- Sriram K**, Insel PA. 2018. G Protein-Coupled receptors as targets for approved drugs: how many targets and how many drugs? *Molecular Pharmacology* **93**:251–258. DOI: <https://doi.org/10.1124/mol.117.111062>, PMID: 29298813
- Stoeber M**, Jullié D, Lobingier BT, Laeremans T, Steyaert J, Schiller PW, Manglik A, von Zastrow M. 2018. A genetically encoded biosensor reveals location Bias of opioid drug action. *Neuron* **98**:963–976. DOI: <https://doi.org/10.1016/j.neuron.2018.04.021>, PMID: 29754753
- Stols L**, Gu M, Dieckman L, Raffin R, Collart FR, Donnelly MI. 2002. A new vector for high-throughput, ligation-independent cloning encoding a tobacco etch virus protease cleavage site. *Protein Expression and Purification* **25**:8–15. DOI: <https://doi.org/10.1006/prep.2001.1603>, PMID: 12071693
- Strickland D**, Lin Y, Wagner E, Hope CM, Zayner J, Antoniou C, Sosnick TR, Weiss EL, Glotzer M. 2012. TULIPs: tunable, light-controlled interacting protein tags for cell biology. *Nature Methods* **9**:379–384. DOI: <https://doi.org/10.1038/nmeth.1904>, PMID: 22388287
- Urban DJ**, Roth BL. 2015. DREADDs (designer receptors exclusively activated by designer drugs): chemogenetic tools with therapeutic utility. *Annual Review of Pharmacology and Toxicology* **55**:399–417. DOI: <https://doi.org/10.1146/annurev-pharmtox-010814-124803>, PMID: 25292433
- Warden MR**, Cardin JA, Deisseroth K. 2014. Optical neural interfaces. *Annual Review of Biomedical Engineering* **16**:103–129. DOI: <https://doi.org/10.1146/annurev-bioeng-071813-104733>, PMID: 25014785
- Watts VJ**, Neve KA. 2005. Sensitization of adenylate cyclase by galpha i/o-coupled receptors. *Pharmacology & Therapeutics* **106**:405–421. DOI: <https://doi.org/10.1016/j.pharmthera.2004.12.005>, PMID: 15922020
- Wedegaertner PB**, Chu DH, Wilson PT, Levis MJ, Bourne HR. 1993. Palmitoylation is required for signaling functions and membrane attachment of Gq alpha and Gs alpha. *The Journal of Biological Chemistry* **268**:25001–25008. PMID: 8227063
- Yang J**, Yan R, Roy A, Xu D, Poisson J, Zhang Y. 2015. The I-TASSER suite: protein structure and function prediction. *Nature Methods* **12**:7–8. DOI: <https://doi.org/10.1038/nmeth.3213>, PMID: 25549265
- Zayner JP**, Antoniou C, French AR, Hause RJ, Sosnick TR. 2013. Investigating models of protein function and allostery with a widespread mutational analysis of a light-activated protein. *Biophysical Journal* **105**:1027–1036. DOI: <https://doi.org/10.1016/j.bpj.2013.07.010>, PMID: 23972854
- Zimmerman SP**, Kuhlman B, Yumerefendi H. 2016. Engineering and application of LOV2-Based photoswitches. *Methods in Enzymology* **580**:169–190. DOI: <https://doi.org/10.1016/bs.mie.2016.05.058>, PMID: 27586333

Appendix 1

Appendix 1—key resources table

Reagent type (species) or resource	Designation	Source or reference	Identifiers	Additional information
Strain, strain background (<i>Escherichia coli</i>)	BL21(DE3)	Invitrogen	Cat# C600003	
Strain, strain background (<i>Escherichia coli</i>)	DH5alpha	New England Biolabs	Cat# C29871	
Genetic reagent (<i>Saccharomyces cerevisiae</i>)	CY7967 [MAT α GPA1(1–41)-Gai3 far1 Δ fus1p-HIS3 can1 ste14:trp1:LYS2 ste3 Δ lys2 ura3 leu2 trp1 his3]	Cismowski et al., 1999		Provided by James Broach (Penn State University)
Cell line (<i>Homo sapiens</i>)	HEK293T cells	ATCC	CRL3216	
Antibody	α -tubulin (mouse monoclonal)	Sigma	T6074	Immunoblotting Dilution (1: 2,500)
Antibody	FLAG tag (mouse monoclonal)	Sigma	F1804	Immunoblotting Dilution (1: 2,000)
Antibody	His-tag (mouse monoclonal)	Sigma	H1029	Immunoblotting Dilution (1: 2,500)
Antibody	Hemagglutinin (HA) tag (clone 12CA5) (mouse monoclonal)	Roche	Cat# 11583816001	Immunoblotting Dilution (1: 1,000)
Antibody	MYC-tag (9B11) (mouse monoclonal)	Cell Signaling	Cat# 2276	Immunoblotting Dilution (1: 1,000)
Antibody	G α s (C-18) (rabbit polyclonal)	Santa Cruz Biotechnology	Cat# sc-383	Immunoblotting Dilution (1: 500)
Antibody	Goat anti-rabbit Alexa Fluor 680 (goat polyclonal)	Life Technologies	Cat# A21077	Immunoblotting Dilution (1:10,000)
Antibody	Goat anti-mouse IRDye 800 (goat polyclonal)	LiCor	Cat# 926–32210	Immunoblotting Dilution (1:10,000)
Recombinant DNA reagent	pLIC-GST (plasmid)	Cabrita et al., 2006		Provided by John Sondek (University of North Carolina- Chapel Hill)
Recombinant DNA reagent	pLIC-GST-LOV2GIV (plasmid)	This paper		
Recombinant DNA reagent	pLIC-GST-LOV2GIV (L) (plasmid)	This paper		Contains the dark-mimicking mutation C450S
Recombinant DNA reagent	pLIC-GST-LOV2GIV (D) (plasmid)	This paper		Contains the dark-mimicking mutation C450S

Continued on next page

Appendix 1—key resources table continued

Reagent type (species) or resource	Designation	Source or reference	Identifiers	Additional information
Recombinant DNA reagent	pLIC-GST-LOV2GIVa (D) (plasmid)	This paper		Contains the dark-mimicking mutation C450S
Recombinant DNA reagent	pLIC-GST-LOV2GIVb (D) (plasmid)	This paper		Contains the dark-mimicking mutation C450S
Recombinant DNA reagent	pLIC-GST-LOV2GIVc (D) (plasmid)	This paper		Contains the dark-mimicking mutation C450S
Recombinant DNA reagent	pLIC-GST-LOV2GIVd (D) (plasmid)	This paper		Contains the dark-mimicking mutation C450S
Recombinant DNA reagent	pLIC-GST-LOV2GIVe (D) (plasmid)	This paper		Contains the dark-mimicking mutation C450S
Recombinant DNA reagent	pLIC-GST-LOV2GIVe (L) (plasmid)	This paper		Contains the lit-mimicking mutation I539E
Recombinant DNA reagent	pLIC-GST-LOV2GIVe (D) (plasmid)	This paper		Contains the dark-mimicking mutation C450S
Recombinant DNA reagent	pLIC-GST-LOV2GIVe (L + FA) (plasmid)	This paper		Contains the lit-mimicking mutation I539E and the GEF-deficient mutation F1685A
Recombinant DNA reagent	pET28b-G α i3 (plasmid)	Garcia-Marcos et al., 2009		For the bacterial expression of rat His-G α i3
Recombinant DNA reagent	pET28b-G α o (plasmid)	Garcia-Marcos et al., 2010		For the bacterial expression of rat His-G α o (isoform A)
Recombinant DNA reagent	pLIC-His (plasmid)	Stols et al., 2002		
Recombinant DNA reagent	pLIC-His- G α i1 (int. 6xHis) (plasmid)	This paper		For the bacterial expression of rat G α i1 with an internal His-tag
Recombinant DNA reagent	pET28b-G α i2 (plasmid)	This paper		For the bacterial expression of rat His-G α i2
Recombinant DNA reagent	p3XFLAG-CMV10-G α i3 (plasmid)	Garcia-Marcos et al., 2009		For the mammalian expression of rat FLAG-G α i3
Recombinant DNA reagent	pcDNA3.1(+)-G α s (plasmid)	Beas et al., 2012		For the mammalian expression of human G α s
Recombinant DNA reagent	pcDNA3-G α q-HA (plasmid)	Wedegaertner et al., 1993		For the mammalian expression of mouse G α q with an internal HA tag. Provided by P. Wedegaertner (Thomas Jefferson University)

Continued on next page

Appendix 1—key resources table continued

Reagent type (species) or resource	Designation	Source or reference	Identifiers	Additional information
Recombinant DNA reagent	pcDNA3.1-Gα12-MYC (plasmid)	Ritchie et al., 2013		For the mammalian expression of mouse Gα12 with an internal MYC-tag. Provided by T. Meigs (University of North Carolina, Asheville)
Recombinant DNA reagent	pLIC-YES2 (plasmid)	Coleman et al., 2016		
Recombinant DNA reagent	pLIC-YES2-N9Gpa1 (plasmid)	Coleman et al., 2016		
Recombinant DNA reagent	pLIC-YES2-LOV2GIVe wt (plasmid)	This paper		For the yeast expression of cytosolic LOV2GIVe
Recombinant DNA reagent	pLIC-YES2-LOV2GIVe (L) (plasmid)	This paper		For the yeast expression of cytosolic LOV2GIVe bearing the lit-mimicking mutation I539E
Recombinant DNA reagent	pLIC-YES2-LOV2GIVe (D) (plasmid)	This paper		For the yeast expression of cytosolic LOV2GIVe bearing the dark-mimicking mutation C450S
Recombinant DNA reagent	pLIC-YES2- N9Gpa1- LOV2GIVe wt (plasmid)	This paper		For the yeast expression of membrane-anchored (m)LOV2GIVe
Recombinant DNA reagent	pLIC-YES2- N9Gpa1- LOV2GIVe (L) (plasmid)	This paper		For the yeast expression of membrane-anchored (m)LOV2GIVe bearing the lit-mimicking mutation I539E
recombinant DNA reagent	pLIC-YES2- N9Gpa1- LOV2GIVe (D) (plasmid)	This paper		For the yeast expression of membrane-anchored (m)LOV2GIVe bearing the dark-mimicking mutation C450S
Recombinant DNA reagent	pLIC-myc (plasmid)	Cabrita et al., 2006		Provided by John Sondek (University of North Carolina- Chapel Hill)
Recombinant DNA reagent	pLIC-lyn11-myc (plasmid)	This paper		
Recombinant DNA reagent	pLIC-lyn11-myc- LOV2GIVe (plasmid)	This paper		For the mammalian expression of mLOV2GIVe
Recombinant DNA reagent	pLIC-lyn11-myc- LOV2GIVe (L) (plasmid)	This paper		For the mammalian expression of mLOV2GIVe bearing the lit-mimicking mutation I539E

Continued on next page

Appendix 1—key resources table continued

Reagent type (species) or resource	Designation	Source or reference	Identifiers	Additional information
Recombinant DNA reagent	pLIC-lyn11-myc-LOV2GIVe (D) (plasmid)	This paper		For the mammalian expression of mLOV2GIVe dark-mimicking mutation C450S
Recombinant DNA reagent	pLIC-lyn11-myc-LOV2GIVe (FA) (plasmid)	This paper		For the mammalian expression of mLOV2GIVe GEF-deficient mutation F1685A
Recombinant DNA reagent	pLIC-lyn11-myc-LOV2GIVe (L) (FA) (plasmid)	This paper		For the mammalian expression of mLOV2GIVe lit-mimicking mutation I539E and the GEF-deficient mutation F1685A
Recombinant DNA reagent	pcDNA3.1-Venus(155-239)-Gβ ₁ (plasmid)	Hollins et al., 2009		For the mammalian expression of Gβ ₁ tagged with a fragment of Venus (VC-Gβ ₁). Provided by N. Lambert (Augusta University, GA)
Recombinant DNA reagent	pcDNA3.1-Venus(1-155)-Gγ ₂ (plasmid)	Hollins et al., 2009		For the mammalian expression of Gγ ₂ tagged with a fragment of Venus (VN-Gγ ₂). Provided by N. Lambert (Augusta University, GA)
Recombinant DNA reagent	pcDNA3.1-Gβ ₁ (plasmid)	Hollins et al., 2009		For the mammalian expression of untagged Gβ ₁ . Provided by N. Lambert (Augusta University, GA)
Recombinant DNA reagent	pcDNA3.1-Gγ ₂ (plasmid)	Hollins et al., 2009		For the mammalian expression of untagged Gγ ₂ . Provided by N. Lambert (Augusta University, GA)
Recombinant DNA reagent	pcDNA3-Gαi3 (plasmid)	Garcia-Marcos et al., 2010		For the mammalian expression of rat Gαi3
Recombinant DNA reagent	pcDNA3.1-masGRK3ct-Nluc (plasmid)	Masuhō et al., 2015		Provided by K. Martemyanov (Scripps Research Institute, FL)
Recombinant DNA reagent	pcDNA3.1-Nluc-EPAC-VV (plasmid)	Masuhō et al., 2015		Provided by K. Martemyanov (Scripps Research Institute, FL)
Recombinant DNA reagent	pcDNA3.1-3xHA-M4R (plasmid)	cDNA Resource Center at Bloomsburg University	Cat# MAR040TN00	

Continued on next page

Appendix 1—key resources table continued

Reagent type (species) or resource	Designation	Source or reference	Identifiers	Additional information
Commercial assay or kit	QuikChange II Site-Directed Mutagenesis Kit	Agilent	Cat# #200523	
Chemical compound, drug	NanoGlo Luciferase Assay System	Promega	Cat# N1120	
Chemical compound, drug	Carbachol	Acros Organics	Cat# AC-10824	
Chemical compound, drug	Atropine	Alfa Aesar	Cat# A10236	
Chemical compound, drug	DL-isoproterenol hydrochloride	Alfa Aesar	Cat# J61788	
Chemical compound, drug	[γ - ³² P]GTP	Perkin Elmer	NEG004Z250UC	
Chemical compound, drug	[³² S]GTP γ S	Perkin Elmer	NEG030H250UC	
Chemical compound, drug	Fluorescein di- β -D-galactopyranoside (FDG)	Marker Gene Technologies	Cat# M0250	
Software, algorithm	I-TASSER	Yang et al., 2015	https://zhanglab.ccmb.med.umich.edu/I-TASSER/	Homology modeling server
Software, algorithm	ICM version 3.8–3	Molsoft LLC., San Diego, CA		Protein structure visualization software